Applied Composite Materials **10:** 19–48, 2003.

E-Glass/Vinylester Composites in Aqueous Environments – I: Experimental Results

V. M. KARBHARI and S. ZHANG
Department of Structural Engineering, MC-0085, University of California, San Diego La Jolla, CA 92093-0085, U.S.A. e-mail: vkarbhari@ucsd.edu

(Received 8 November 2000; accepted 11 March 2002)

Abstract. 2- and 4-layered specimens of E-Glass/Vinylester fabricated from uniaxial, biaxial, and triaxial, non-woven fabrics processed using the resin infusion process are immersed in deionized water at 23 °C (73 °F) and 60 °C (140 °F), and a potassium based pH 10 buffer at 73 °F, for a period of 57 weeks in order to investigate durability in aqueous environments. It is shown that the coefficients of apparent diffusion and levels of moisture gain are the highest for the deionized water immersed samples at 60 °C (140 °F), and this results in the highest levels of tensile strength and modulus degradation. Tensile tests show the presence of an aqueous medium based post-cure that competes with the conventionally recognized mechanisms of deterioration in the resin, at the level of the fiber-matrix interface, and in the fiber, resulting in a retardation of absolute level of effects. It is also shown that effects of the immersion are different in the warp and fill directions and can in fact be affected by intricacies of the fabric architecture and thickness. It is shown that damage takes place through interface debonding and degradation as well as fiber pitting, and cracking, each of which serve as the means for renewed absorption of water resulting in moisture uptake at levels above the initial plateau. Effects of immersion on short-beam-shear strength and glass transition temperature are also elucidated.

Key words: E-glass, vinylester, fabric architecture, resin infusion, fiber cracking, interphase degradation, pitting.

1. Introduction

Due to considerations of cost and levels of ultimate strain achievable, E-glass fibers are often preferred to carbon fibers despite their significantly lower modulus and higher susceptibility to environmentally induced degradation. In similar fashion, resin systems, such as polyesters and vinylesters, cured under ambient temperature conditions are often used, in preference to higher performance elevated temperature cure epoxy systems, due to considerations of cost and ease of processability. This is especially true in the fast growing area of civil infrastructure where fiber reinforced polymer (FRP) composites are increasingly being considered, and used, for primary load bearing components such as bridge decks, and in full structural systems. Their use in these applications necessitates an assurance of long-term durability after exposure to environmental conditions likely to be faced over the expected lifetime of the structure.

Although there is substantial anecdotal evidence of the longevity of some composites, there is currently a lack of information for a number of systems, including E-glass/vinylesters, to a level sufficient to prove actual durability over extended (50+ years) time periods under sustained load and cyclic fatigue conditions, or to enable reasonable predictions to be made on the basis of well substantiated and validated data bases [1]. Schutte [2], in a recent survey, and Weitsman [3] have emphasized the lack of assimilation of data related to durability, even as related to common regimes such as aqueous environments. The lack of data on such systems can partly be ascribed to the consideration, in the past, of glass-fiber composites being considered as "low-tech" leading to the use of very conservative factors of safety in an attempt to overcome known, but unquantified, detrimental effects. Due to the level of uncertainty, in the marine field partial safety factors of 4–6 are routinely applied "in the design of long-term cyclic loaded structures in dry conditions", with additional factors being used for moisture absorption effects [4]. For the design of corrosion resistant equipment factors as high as 10 are used for strength as related to the determination of minimum thickness for cylindrical shells under internal pressure [5]. Based on a survey of glass reinforced polymer structures Leiblein [6] concluded that for long-term outdoor use (10–30 years) design operating pressures should not exceed 20% of ultimate laminate strength for uncoated pressure vessels.

Since structural composites will, through their design life, be exposed to a range of hygrothermal conditions, the determination of the mechanics of degradation and levels of performance retention are critical for designers. Although significant research has been conducted into determining the effect of moisture absorption on autoclave cured prepreg based composites, there is a much lower level of understanding as related to ambient cured vinylester based systems [1, 7, 8]. It is important to note that in general these are comprised of low molecular weight polyhydroxyether chains with reactive groups at chain ends. Styrene in the monomeric form is used as a diluent in the resin in quantities between 20% and 60%. Although increases in styrene content can result in increases in hydrophobicity (and thus an effective decrease in the level of moisture absorption) it also results in an increase in shrinkage (resulting in the potential for significant microcracking in resin rich areas and high residual stresses in composites having high fiber volume fractions) as well as the possibility of incomplete polymerization. Incomplete polymerization not only leads to changes in properties with time due to slow changes in degree of cure, but also induces lower heat stability, lower resistance to hydrolysis and a greater degree of susceptibility of swelling in solvents [9]. In addition, the hydrolysis of ester groups can result in the formation of carboxyl groups, resulting in further decomposition due to autocatalysis [10].

In evaluating the applicability of composites for use in primary structural elements, such as bridge decks for civil infrastructure applications, the assessment of effects of aqueous and hygrothermal exposure are critical. This is even more

Table I. Details of fabrics.

Designation	Fabric type	Basis weight g/m^2 (oz/sq. yd.)	Fabric construction* Warp	Fill	Bias (±45)
UM2403	Uniaxial	814 (24)	9 epi[1] 225 yield[2] 1 epi 450 yield 24 oz 10 ga[3]		
CM5005	Biaxial	1695 (50)	10 epi 225 yield 25.5 oz 7 ga	7.84 epi 225 yield 6.25 epi 675 yield 25.5 oz 7 ga	
TVM348	Triaxial	1153 (34)	3 epi 225 yield 7 epi 450 yield 16 oz 10 ga		0.3 epi 675 yield 8.8 epi 1800 yield 9 oz 10 ga

*Details of fabric construction are provided as manufactured, for purposes of identification, and are hence provided in the imperial system of units, as used. Fabrics have a chopped strand mat backing of 25 g/m^2 (0.75 oz/sq. yd.) basis weight.
[1]epi: ends per inch.
[2]yield: length obtained in yards per pound of input roving.
[3]ga: gauge, i.e. rows of stitching across the roll width.

important since effects of fluid sorption are highly dependent on the specifics of the constituent materials, their combination through the selected process steps, the details of fabric architecture involved, and the level of surface protection afforded through the use of gel coats, veils etc. This paper reports on aspects related to exposure of E-glass/vinylester composites fabricated with three multi-axial non-woven stitched reinforcement architectures using the resin infusion process. The study is part of an on-going investigation aimed at the characterization and modeling of environmental durability of material sets likely to be used in civil infrastructure applications, and the development of life-prediction methodologies for these materials combining effects of post-cure and completion of polymerization over time with physiochemical effects of degradation and aging.

2. Materials Systems and Test Procedures

For the purposes of the current study E-glass/vinylester composites were fabricated using the resin infusion process. E-glass fibers in non-woven fabric form in uniaxial, biaxial and triaxial architectures (as detailed in Table I) were infused under ambient conditions (75 °F, 56% RH) using a Dow Derakane 411–350 Vinylester

system* catalyzed by Cobalt Napthenate and Cumene Hydroperoxide using nominal weight fractions of 0.3% and 3% respectively. The fabrics essentially consist of appropriately oriented layers of unidirectional yarn bound to one another using stitching thread. The architectures considered in this investigation are the uniaxial (consisting of a layer with all fibers in one direction), biaxial (consisting of two layers, one at 0 degrees and the other with yarn oriented at 90 degrees, i.e. perpendicular to the direction of the first layer) and triaxial (consisting of three layers oriented at 0 degree, −45 degrees and +45 degrees, respectively). Schematics of the three stitched non-woven fabrics are shown in Figure 1. As noted in Table I the fabrics had a backing of chopped strand mat of 25 g/m^2 (0.75 oz/sq. yd.) which enhanced both handlability and wet-out. After infusion, the panels, which were fabricated in thicknesses of two and four layers of each of the fabric types, were allowed to cure for 24 hours at 23 °C (73 °F) and 56% RH after which they were postcured at 93 °C (200 °F) for 2 hours.

Specimens for tension (per ASTM 3039) and short-beam shear (per ASTM D790M-84) testing were cut, using a water-cooled diamond tipped saw blade, from each panel in both the primary warp (machine direction, i.e. along the primary unidirectional yarn) and fill (perpendicular to the machine direction, i.e. perpendicular to the unidirectional yarn) directions. In addition further specimens of 25 × 25 mm size were cut for moisture absorption studies. After cutting, each sample was sealed on all edges using the same resin system used for infusion. After conditioning, specimens were immersed in deionized water at 23 °C (73 °F) and 60 °C (140 °F), and a potassium based buffer at pH 10 at 23 °C (73 °F). The elevated temperature level was chosen for purposes of accelerated testing with the temperature level chosen being representative of the highest level of temperature likely to be seen during the service life of a composite structure used in civil infrastructure applications under normal conditions. The temperature also represents a level beyond which the combined effects of moisture ingress and temperature would result in a change in damage mechanisms and is hence often assumed to be the highest safe level of accelerated testing through time–temperature superposition principles. Tests were conducted on each set of specimens (consisting of a minimum of 5 replicates) after time periods of 1 week, 4 weeks, 8 weeks, 12 weeks, 28 weeks, and 57 weeks of exposure, with tests also being conducted on equivalent specimen sets kept at 75 °F and 56% RH to provide a constant assessment of "unexposed" response. These specimens were tested at each time period and results used as the control basis for each set to incorporate results of slow ambient post/residual-cure, and the resulting changes in properties as indicated in [11–13]. This is important since vinylester systems do not undergo complete polymerization, even after short periods of elevated temperature post-cure, resulting in gradual changes in levels of performance with time.

* Identification of material by commercial designation is for purposes of adequate specification and documentation only. Such identification is not intended to imply recommendation or endorsement.

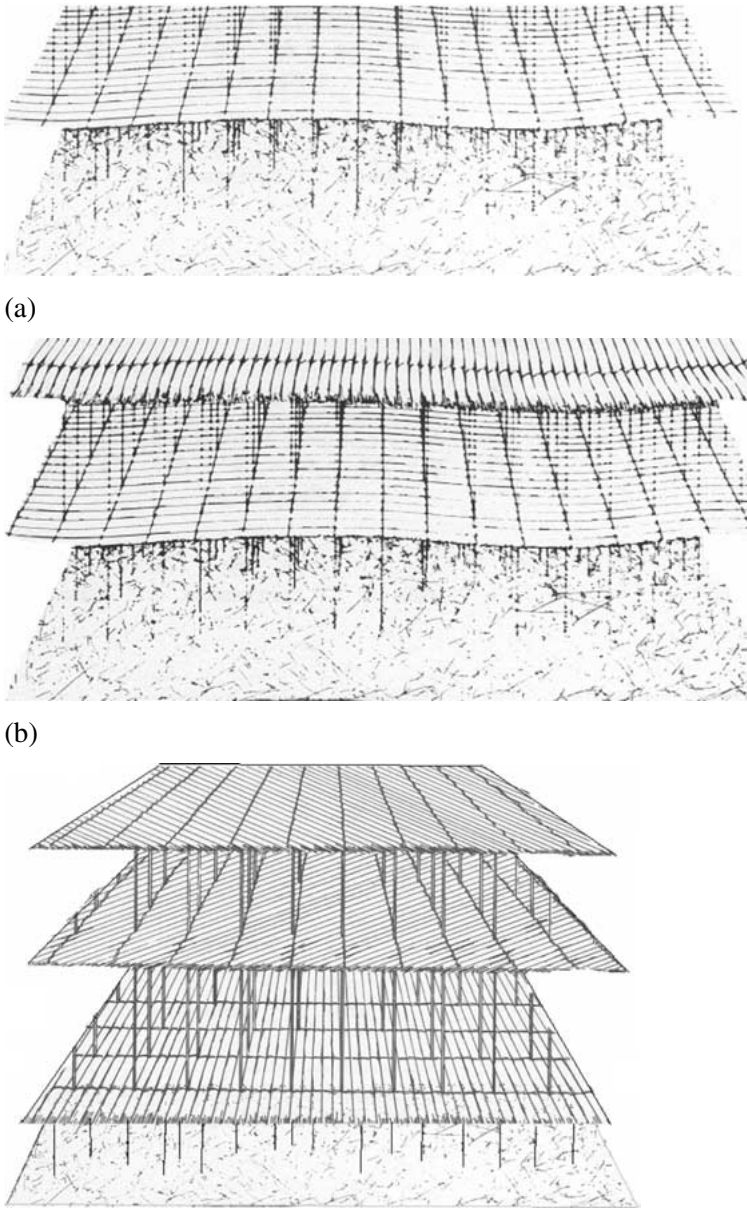

Figure 1. Schematic of multi-axial nonwoven stitched fabric: (a) uniaxial; (b) biaxial; (c) triaxial.

3. Results and Discussion

Burnoff procedures (consisting of heating a preweighed sample of composite in a heat resistant crucible at 625 °C until the charred residue of the resin has been

removed, and then weighing the fibrous residue after cooldown following procedures in ISO 1172, and determining volume fraction from the weight fraction so obtained) on representative samples showed that the composites had fiber volume fractions between 52–55% with no discernible difference on the basis of thickness or fabric architecture. Microscopic analysis, using a quantitative analysis microscope with image processing software incorporating grey scales, indicated that void fractions ranged between 2–4%, again with no specific effects of thickness or fabric architecture. Within the two layered set, the unidirectional specimens had a nominal thickness of 1.6 mm, the bi-directional ones had a nominal thickness of 2.9 mm, and the triaxial specimens had a thickness of 2.5 mm. Within the four layered set, the unidirectional specimens had a nominal thickness of 3.0 mm, the bi-directional ones had a nominal thickness of 5.6 mm, and the triaxial specimens had a thickness of 4.5 mm. This clearly shows that the increase in thickness is not linear with the number of layers, due to reasons of local compaction and interpenetration of fibers from adjacent layers. As shown in Table I the nominal areal weight (basis weight) for each direction in the fabrics is not the same and hence a direct comparison on the basis of unit compaction is not possible.

3.1. MOISTURE ABSORPTION

It is important to clarify that mass uptake due to immersion in liquids can occur through both absorption and adsorption. While the former is a bulk effect, the latter can be considered a surface effect. Absorption occurs through capillary uptake through voids, microcracks and interface gaps, resulting in the filling of free space without immediate plasticization or swelling [14]. In contrast the process of adsorption generates heat and results in swelling. In the case of polymers (and their composites) which inherently contain defects both processes are likely [14] and hence the term moisture uptake to represent the combination of these processes is more appropriate. Penetrant uptake, in terms of weight gain was determined through gravimetric sorption. The weight gain in each of the three environments was carefully monitored through periodic assessment with precautions taken to remove surface moisture by carefully wiping each specimen before weighing. Percentage weight gain was determined as

$$M = \left(\frac{\text{Weight of specimen} - \text{Weight of dry specimen}}{\text{Weight of dry specimen}} \right) \times 100.$$

A typical trace of mass uptake in the neat resin and the three composites is shown in Figure 2. Comparing mass uptake differences between specimens immersed in deionized water at 23 °C (73 °F) and 60 °C (140 °F) it was noted that the rate of approach to the initial equilibrium plateau is about 20% higher at the elevated temperature relative to that at 23 °C (73 °F). Mass uptake is also higher (as reported in Table II) which can be related to effects of both adsorption and absorption causing swelling of the polymer in addition to hygrothermal aging which leads to damage

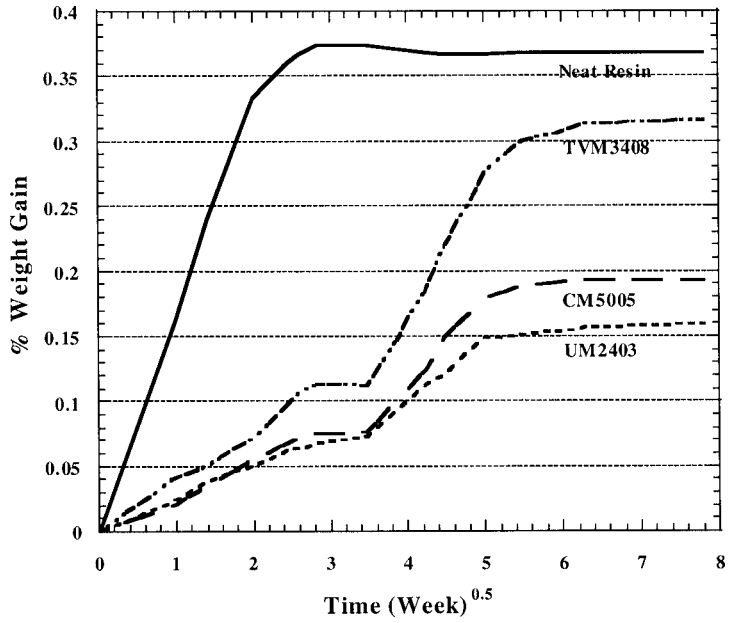

Figure 2. Weight gain profiles for neat resin and two-layered specimens in deionized water at 73 °F as a function of time.

formation in the form of surface microcracking, discoloration, jackstrawing (similar to that reported in [15]), volume microcracking, microcrack coalescence to form a transverse crack (Figure 3), fiber-matrix debonding and changes in the bulk (Figure 4), all of which enable additional sorption to occur. It can also be seen that the level of absorption increases with the number of base fabric orientations with the minimum weight gain being shown by the uniaxial specimens and the maximum by the triaxially reinforced specimens. Since fiber volume fractions of the material are roughly equivalent the effect can be hypothesized to be due to absorption along fiber-resin interfaces with increased directionality resulting in increased

Table II. Comparison of apparent diffusivity and percentage weight gain.

Specimen	Deionized water at 23 °C		Deionized water at 60 °C		pH 10 buffer solution	
	% Weight gain	Apparent diffusivity ($\times 10^{-7}$ mm^2/s)	% Weight gain	Apparent diffusivity ($\times 10^{-7}$ mm^2/s)	% Weight gain	Apparent diffusivity ($\times 10^{-7}$ mm^2/s)
Neat resin	0.37	7.9	0.65	11.5	0.22	6.8
UM2403	0.16	4.5	0.25	7.6	0.10	3.2
CM5005	0.19	4.7	0.31	8.0	0.16	4.3
TWM3408	0.32	4.8	0.50	8.5	0.20	4.6

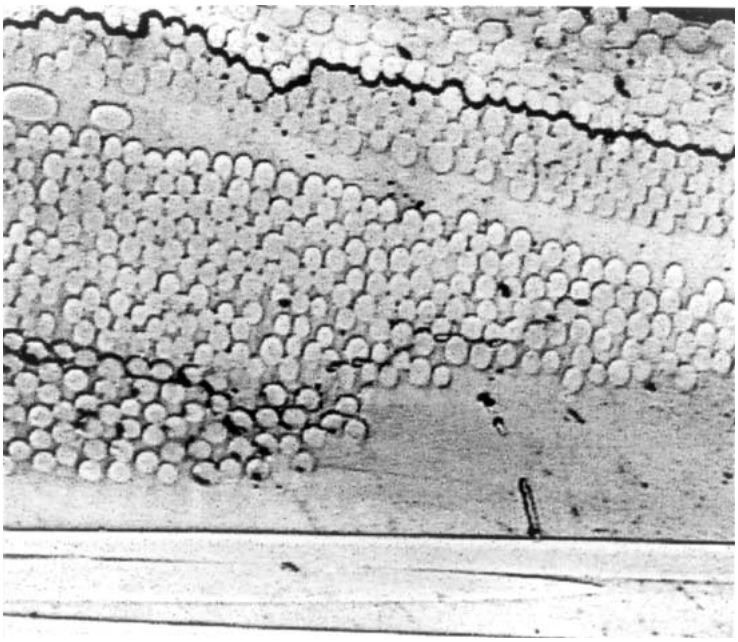

Figure 3. Interfacial debonding and formation of a macro-crack after immersion in deionized water at 140 °F.

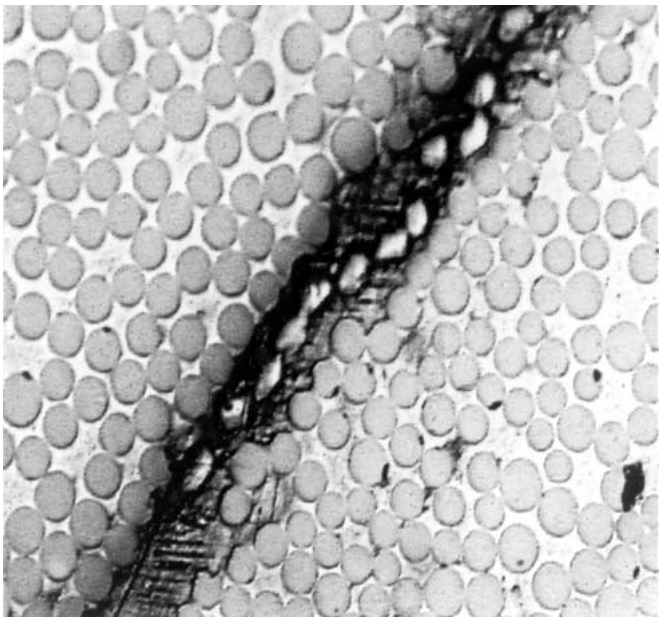

Figure 4. Morphological change in bulk resin in a band between fibers in a layered specimen after immersion in deionized water at 140 °F for 57 weeks.

interfaces, and cross-over or contact points. In all cases for the composite, moisture absorption profiles showed evidence of a two-stage process with the attainment of an initial plateau followed by renewed weight gain and the attainment of a second more stable plateau at higher levels of weight gain. This type of response has been noted previously in glass fiber/vinylester composites [16], glass/polyester composites [17] and SMC [18] of both polyester and vinylester, and follows the general trends described for brittle materials [19]. This type of response can be traced either to the changing viscoelastic response proposed by Weitsman [20] in which boundary conditions change with time resulting in anomalous or pseudo-Langmuir type response, or more plausibly to a combination of (a) effects related to relaxation of elastic forces exerted by the cross-linked network after initial moisture gain, and (b) degradation at the fiber-matrix interphase and fiber levels which starts after the initial plateau period allowing for significant wicking and further increase in absorption. It should be noted that the "two-stage" diffusion behavior has previously been explained as being due to a portion of the diffusing fluid being entrapped and reduced to immobility within the polymer itself, whereas the remainder remains mobile and continues to diffuse through the material [20–22]. It is noted that in vinylester systems moisture uptake can be accompanied by residual cure or by a chemical reaction [3], however, the actual deviation from classical diffusion distributions are insignificant at the global level [3], and can be approximated by classical diffusion distributions [23, 24].

Assuming, then, that in the global sense, moisture absorption follows Fick's law (i.e. neglecting the short period of initial plateau as a local anomaly, or as in this investigation as a result of chemical reaction), the apparent diffusivity, D, as an approximation of relative behavior, can be determined as [25]

$$D = \pi \left(\frac{h}{4M_m} \right)^2 \left(\frac{M_2 - M_1}{\sqrt{t_2} - \sqrt{t_1}} \right)^2 \left(1 + \frac{h}{L_e} + \frac{h}{w} \right)^{-2},$$

where L_e, W, and h are the length, width and thickness of the test specimen, respectively, and M_1 and M_2 are moisture contents at times t_1 and t_2, respectively. Both t_1 and t_2 are such that weight change can still be assumed to vary linearly with the square root of time. Values for maximum moisture content (recorded as percentage weight gain) achieved within the time period of exposure and apparent diffusivity are given in Table II. As with the percentage weight gain, apparent diffusivity values also increase with the number of bias orientations. The value of diffusivity for the neat vinylester specimens immersed in water at 73 °F are consistent with those reported by Marshall *et al.* [16] of 8.2×10^{-7} mm^2/s and Harper and Naeem [7] on a similar Dow Derakane 411 series vinylester of 6.76×10^{-7} mm^2/s. It is of interest to note that Harper and Naeem [7] reported a value of D of 1.145×10^{-6} mm^2/s for the 411 series vinylester when immersed in water at 140 °F, which compares very closely to the value of 1.15×10^{-6} mm^2/s determined for the same condition in the current investigation. In a recent study of durability of a UM2403 based vinylester composite exposed to a range of concrete based alkaline solutions Zhang

and Karbhari [26] had reported apparent diffusivity coefficients for the composite between 4.13×10^{-7} mm^2/s and 6.45×10^{-7} mm^2/s depending on the alkali solution under consideration, and a value of 4.69×10^{-7} mm^2/s for the composite immersed in deionized water, for a period of 18 months. Whereas the values determined after immersion in deionized water in the two studies differ by only 4%, there is a greater difference due to the alkali solution used, emphasizing the importance of solution chemistry effects in such studies. As was discussed in [26] and will be described later, this also shows the importance of appropriate simulation of environments since the use of a potassium buffer although at a high pH level (pH 10) does not duplicate effects of a concrete based alkali solution, and/or concrete pore water, due to differences in solution chemistry and the resultant diffusion of salt bearing solutions through a composite.

The activation energy for diffusion, E_d, can be determined using an Arrhenius type of relationship [19]

$$D = D_0 \exp\left(\frac{-E_d}{RT}\right),$$

where D_0 is a constant coefficient, R is the universal gas constant (8.3143 J/mol °K) and T is the temperature measured on the Kelvin scale. Using the data for deionized water in Table II, and results of additional moisture uptake tests conducted in deionized water at 40 °C wherein the apparent diffusivities for the neat resin, UM2403 composite, CM5005 composite and the TVM3408 composite, were found to be 6.05×10^{-7} mm^2/s, 6.2×10^{-7} mm^2/s, and 6.7×10^{-7} mm^2/s, respectively, for a plot of $\ln(D)$ versus $(1/T)$, values of the activation energy determined from the slope of the line were 8270 J/mol, 11540 J/mol, 11715 J/mol and 21585 J/mol for the neat resin, UM2403 based composite, CM5005 based composite, and TVM3408 based composite, respectively. The lower activation energy of the neat resin indicates a weaker diffusion barrier and consequently greater absorption. It is noteworthy that the unidirectional and biaxial composites do not show a significant change in activation energy level, whereas the triaxial has the highest level. Due to the presence of the layer of mat in each fabric layer there is substantial interpenetration of fibers between layers during compaction and hence resin rich layers do not as such exist, as they would in prepreg based composites, in the specimens fabricated by resin infusion. The apparent discrepancy in trends between the mass uptake levels and activation energy in the TVM3408 composites is perhaps related to orientation and difference in basis weight of the different orientation layers (47% of the basis weight is in the warp direction, with 26.5% being in each of the bias directions) as well as the fact that the sizing used on the basis layers of the triaxial was different from that of the 0 degree layer, which results in different surface interactions as reported in [27], and hence in reality the diffusion coefficients reported in Table II need to be considered as average values since in-plane diffusivities would be different in the orientation directions since the triaxial does not constitute a balanced equal weight layup configuration.

3.2. TENSILE CHARACTERIZATION

Overall results of tensile characterization, strength and modulus, are listed in Tables III–VI. It can be seen that in all cases immersion in the three environments results in a decrease in both strength and modulus. As can be seen from Tables III and IV the maximum drop in strength is seen after immersion in deionized water at 60 °C (140 °F), and as shown in Figure 5, the drop in strength after 60 °C (140 °F) immersion is significantly greater, over the time period under consideration, than from the other two solutions, which is in line with previous investigations on the use of elevated temperature as a means of acceleration. It is noted from Tables III and IV and Figure 5 that the reduction in tensile strength is higher in the warp direction than in the fill (i.e. weft) direction, even for the unidirectional composites indicating that the changes are not merely associated with plasticization and hydrolysis of the resin, but also with degradation at the level of the fiber–matrix interface (Figure 6a) and that of the individual fiber itself (Figure 6b). The pitting seen in these figures is due to a loss of K_2O and Na_2O from the fiber by dissolution, which was earlier identified by Wyatt and Ashbee [28] and further validated by Ishai [29] through infrared analysis of leached components to identify leached elements in the solution, as was in the present study. The axial cracking in the fiber as seen in Figure 6b is representative of damage at elevated temperatures and was noted earlier by Ehrenstein and Spaude [30]. The degradation in the glass fibers in the current investigation is hypothesized to be caused by condensed water, in contrast to individual molecules, which diffuses/penetrates along debonded and cracked fiber-matrix interfaces. The silanol end of the coupling agent reacts with a hydrated oxide on the glass surface, with the rate of reaction increasing with temperature until an initial equilibrium is reached.

In the case of the 2 layered biaxial specimens it is seen that the coupons cut along the warp direction show a lower percentage retention of strength, 72.6%, than those cut in the fill direction, 87.7%, despite the fabric architecture being nominally a balanced one. It is however noted from Table I that the details of fabric construction are not the same in the warp and fill and the larger number of interfaces provide a reason for this discrepancy. It is also noted that this is not seen at the 4 layer level which could either be due to the longer time period required for equivalent moisture penetration/diffusion in the thicker composites, or the effect of slower fiber level degradation due to the higher level of compaction and fiber interpenetration seen between layers as the number of layers increases. It should be noted that in resin infused fabric composites, compaction is not linear, but results in increased interpenetration of the layers in the mat within the aligned rovings of the layer adjacent to it, as thickness increases resulting in a straining effect. From Figure 5 it is clear that in the fiber dominated direction (warp) the effect of fiber orientation is significant with the difference, although still discernible, being significantly less in the fill direction.

Penetration of aqueous solutions into thermoset composites is known to cause both plasticization over the short-term and hydrolysis through attack of ester link-

Table III. Overall results of tensile strength (MPa) characterization in the warp direction.

Fabric	Number of layers	Exposure	Time of immersion						
			Unexposed	1 week	4 weeks	8 weeks	12 weeks	26 weeks	57 weeks
UM2403	2	Water at 23 °C	875.7 [8.48]	525.5 [45.64]	649.4 [24.82]	651.0 [28.82]	560.2 [32.96]	465.6 [52.47]	460.5 [5.45]
		Water at 60 °C		537.7 [6.41]	434.0 [46.89]	403.6 [33.51]	374.1 [25.58]	341.3 [33.92]	312.5 [15.31]
		pH 10 buffer		523.9 [101.91]	758.6 [62.68]	780.8 [35.51]	794.0 [12.34]	759.2 [12.41]	675.1 [9.86]
	4	Water at 23 °C	923.9 [65.36]	814.7 [63.43]	638.2 [95.22]	608.3 [122.39]	459.3 [52.13]	371.6 [78.81]	347.9 [31.44]
		Water at 60 °C		814.7 [42.75]	691.9 [20.69]	671.5 [55.92]	487.1 [3.79]	478.9 [17.31]	489.9 [32.75]
		pH 10 buffer		746.3 [65.23]	727.4 [69.50]	673.9 [74.81]	699.1 [73.85]	670.3 [7.93]	676.3 [46.54]
CM5005	2	Water at 23 °C	478.3 [26.55]	451.2 [28.89]	437.7 [21.51]	419.4 [42.34]	400.8 [11.45]	414.5 [30.27]	347.4 [41.3]
		Water at 60 °C		409.9 [10.96]	249.4 [17.65]	218.1 [2.34]	206.4 [10.00]	180.2 [5.65]	153.9 [4.48]
		pH 10 buffer		458.3 [13.24]	422.4 [28.48]	394.3 [42.06]	414.6 [64.54]	365.0 [19.09]	364.0 [33.3]
	4	Water at 23 °C	400.4 [9.31]	370.8 [24.82]	346.5 [7.79]	299.2 [68.81]	367.4 [65.02]	385.1 [51.78]	337.9 [17.79]
		Water at 60 °C		400.4 [9.24]	278.4 [97.50]	246.0 [14.69]	202.4 [12.41]	207.3 [7.58]	161.7 [7.79]
		pH 10 buffer		458.1 [34.61]	448.3 [21.51]	401.9 [21.31]	386.7 [75.02]	444.2 [47.02]	397.8 [29.86]
TVM3408	2	Water at 23 °C	466.4 [33.03]	442.1 [12.82]	453.1 [56.47]	463.3 [46.61]	474.8 [11.03]	407.1 [34.34]	399.4 [27.44]
		Water at 60 °C		344.1 [20.55]	257.6 [27.17]	272.0 [9.93]	220.2 [18.96]	214.8 [28.13]	200.0 [21.51]
		pH 10 buffer		487.1 [31.79]	459.2 [26.20]	450.2 [26.02]	447.6 [52.54]	444.9 [48.54]	448.9 [9.79]
	4	Water at 23 °C	531.1 [27.92]	517.3 [21.31]	459.7 [5.86]	509.2 [14.27]	484.9 [10.62]	452.6 [22.89]	452.1 [26.89]
		Water at 60 °C		410.5 [10.34]	293.5 [8.41]	262.1 [17.31]	246.6 [13.58]	242.0 [11.79]	240.8 [11.58]
		pH 10 buffer		523.1 [10.41]	513.8 [12.76]	457.4 [45.71]	463.1 [8.62]	469.6 [34.96]	460.7 [10.83]

Table IV. Overall results of tensile strength (MPa) characterization in the fill direction.

Fabric	Number of layers	Exposure	Time of immersion						
			Unexposed	1 week	4 weeks	8 weeks	12 weeks	26 weeks	57 weeks
UM2403	2	Water at 23 °C	39.1 [0.83]	34.9 [2.14]	31.8 [7.59]	32.2 [4.62]	34.8 [1.45]	34.7 [1.72]	31.2 [1.17]
		Water at 60 °C		27.7 [2.21]	25.4 [3.72]	29.4 [6.00]	29.7 [2.34]	23.3 [5.52]	20.7 [3.65]
		pH 10 buffer		34.8 [1.24]	34.8 [1.52]	33.1 [2.90]	34.1 [0.83]	30.8 [1.17]	30.5 [4.00]
	4	Water at 23 °C	48.4 [0.48]	51.4 [1.45]	35.7 [2.41]	36.8 [10.76]	44.3 [0.90]	42.4 [4.41]	41.5 [5.72]
		Water at 60 °C		44.1 [2.34]	39.9 [0.41]	45.6 [2.69]	41.9 [1.65]	42.9 [0.55]	41.0 [0.90]
		pH 10 buffer		46.5 [2.62]	44.1 [3.59]	41.6 [12.69]	48.1 [3.17]	43.8 [6.55]	36.4 [11.03]
CM5005	2	Water at 23 °C	414.1 [15.17]	423.5 [11.79]	419.8 [22.13]	441.8 [32.61]	430.0 [41.09]	377.64 [51.30]	363.2 [39.51]
		Water at 60 °C		346.3 [19.58]	263.3 [28.13]	229.7 [13.38]	228.7 [15.44]	227.5 [21.31]	182.4 [21.44]
		pH 10 buffer		443.0 [24.48]	439.6 [12.96]	422.1 [28.68]	438.0 [17.03]	407.3 [27.92]	372.5 [18.41]
	4	Water at 23 °C	419.3 [26.89]	373.0 [14.62]	393.6 [27.37]	368.6 [51.3]	400.4 [39.44]	334.1 [68.05]	332.3 [23.58]
		Water at 60 °C		404.1 [13.38]	275.8 [52.47]	228.0 [17.03]	221.0 [26.55]	189.3 [17.24]	151.7 [15.03]
		pH 10 buffer		387.4 [50.33]	393.1 [26.13]	429.6 [15.93]	365.4 [48.95]	419.6 [35.37]	403.6 [0.34]
TVM3408	2	Water at 23 °C	139.7 [6.55]	130.6 [8.69]	129.9 [6.34]	129.5 [6.34]	133.5 [9.17]	125.4 [2.55]	114.0 [15.51]
		Water at 60 °C		101.2 [4.48]	90.0 [6.14]	73.4 [9.17]	75.4 [12.62]	62.1 [24.48]	54.0 [10.27]
		pH 10 buffer		120.9 [3.93]	133.2 [2.90]	124.5 [8.21]	121.1 [9.45]	125.0 [11.51]	118.6 [6.96]
	4	Water at 23 °C	151.0 [6.62]	142.9 [3.59]	140.2 [1.86]	138.4 [1.79]	144.9 [5.86]	140.0 [8.76]	139.1 [1.59]
		Water at 60 °C		121.9 [3.86]	94.1 [6.69]	98.8 [3.24]	94.2 [3.10]	90.2 [1.72]	89.4 [1.79]
		pH 10 buffer		138.2 [6.69]	148.7 [6.14]	143.4 [4.48]	140.8 [6.07]	143.4 [10.69]	135.7 [9.17]

Table V. Overall results of tensile modulus (GPa) characterization in the warp direction.

Fabric	Number of layers	Exposure	Time of immersion						
			Unexposed	1 week	4 weeks	8 weeks	12 weeks	26 weeks	57 weeks
UM2403	2	Water at 23 °C	36.3 [2.14]	29.3 [1.59]	31.7 [0.34]	32.1 [3.86]	3.4 [0.21]	32.4 [3.17]	32.1 [1.17]
		Water at 60 °C		39.5 [2.62]	33.7 [2.07]	38.2 [4.07]	37.3 [2.34]	33.0 [1.72]	32.1 [0.90]
		pH 10 buffer		35.1 [2.62]	37.9 [3.10]	37.0 [2.69]	37.2 [4.00]	35.7 [0.90]	34.8 [2.34]
	4	Water at 23 °C	42.0 [0.07]	36.8 [0.14]	39.1 [2.00]	40.1 [5.10]	37.4 [5.24]	37.2 [2.41]	36.7 [3.79]
		Water at 60 °C		38.1 [2.90]	35.1 [1.72]	44.8 [6.34]	42.1 [2.83]	43.0 [3.03]	39.6 [3.10]
		pH 10 buffer		35.9 [3.86]	38.3 [2.83]	37.7 [2.34]	35.5 [0.62]	34.5 [2.14]	34.5 [3.45]
CM5005	2	Water at 23 °C	28.1 [7.45]	25.9 [1.72]	25.5 [0.69]	23.7 [1.31]	23.0 [0.90]	22.9 [2.34]	22.8 [2.07]
		Water at 60 °C		23.2 [1.65]	29.9 [2.00]	29.2 [4.83]	21.7 [2.62]	21.7 [3.32]	21.5 [3.86]
		pH 10 buffer		25.7 [1.10]	23.7 [3.31]	26.1 [1.17]	24.1 [0.62]	24.1 [3.79]	20.1 [2.21]
	4	Water at 23 °C	28.9 [0.62]	27.3 [0.97]	27.4 [0.48]	27.4 [1.59]	29.4 [1.45]	28.0 [0.97]	27.5 [0.34]
		Water at 60 °C		25.9 [1.65]	29.4 [2.48]	26.1 [1.17]	25.8 [1.52]	24.5 [1.24]	21.5 [1.45]
		pH 10 buffer		25.8 [0.83]	26.6 [0.69]	28.2 [3.03]	27.4 [4.07]	26.3 [1.38]	25.8 [1.65]
TVM3408	2	Water at 23 °C	27.9 [6.65]	19.0 [1.38]	24.3 [2.28]	23.3 [1.65]	25.0 [0.69]	20.3 [0.48]	21.6 [1.17]
		Water at 60 °C		23.5 [1.24]	24.8 [3.95]	23.9 [1.59]	26.8 [4.83]	24.1 [1.03]	22.4 [0.62]
		pH 10 buffer		24.3 [2.14]	22.9 [0.97]	23.8 [0.69]	23.2 [2.34]	21.1 [2.55]	19.3 [0.34]
	4	Water at 23 °C	23.3 [2.48]	19.9 [1.24]	23.9 [1.31]	24.7 [0.83]	24.3 [1.59]	23.8 [0.83]	22.3 [3.10]
		Water at 60 °C		25.3 [2.00]	25.7 [3.95]	26.4 [2.14]	25.9 [4.55]	23.9 [1.86]	21.6 [0.90]
		pH 10 buffer		24.7 [3.17]	23.5 [0.07]	24.3 [2.41]	24.9 [3.31]	24.5 [0.83]	24.2 [0.55]

Table VI. Overall results of tensile modulus (GPa) characterization in the fill direction.

Fabric	Number of layers	Exposure	Time of immersion						
			Unexposed	1 week	4 weeks	8 weeks	12 weeks	26 weeks	57 weeks
UM2403	2	Water at 23 °C	13.7 [0.55]	11.9 [1.17]	12.8 [0.34]	13.7 [0.34]	11.7 [0.48]	13.5 [0.83]	13.4 [0.14]
		Water at 60 °C		12.8 [0.90]	12.3 [2.00]	12.0 [1.03]	13.1 [1.24]	12.8 [1.52]	12.7 [0.90]
		pH 10 buffer		12.2 [1.03]	12.2 [0.90]	12.0 [3.72]	15.7 [3.59]	13.0 [1.24]	12.1 [1.79]
	4	Water at 23 °C	14.6 [0.14]	12.8 [0.28]	14.6 [2,34]	12.8 [0.6]	14.4 [0.83]	13.3 [0.28]	13.5 [0.76]
		Water at 60 °C		13.7 [0.62]	12.5 [1.17]	14.1 [0.48]	14.8 [0.34]	13.6 [0.76]	12.7 [1.03]
		pH 10 buffer		13.5 [0.34]	15.4 [1.59]	13.7 [0.83]	13.7 [0.62]	15.4 [3.17]	13.6 [0.41]
CM5005	2	Water at 23 °C	26.3 [0.07]	24.6 [1.17]	26.3 [1.65]	26.7 [3.52]	28.3 [2.55]	22.6 [2.48]	23.7 [5.24]
		Water at 60 °C		24.6 [2.48]	28.6 [4.55]	23.1 [1.24]	22.0 [1.03]	21.7 [1.38]	20.8 [0.90]
		pH 10 buffer		25.9 [1.24]	25.7 [0.34]	27.9 [0.41]	24.4 [2.96]	21.7 [1.72]	21.2 [0.90]
	4	Water at 23 °C	25.1 [2.55]	25.3 [1.93]	24.6 [1.24]	25.4 [1.93]	25.6 [2.96]	23.4 [1.31]	23.4 [1.52]
		Water at 60 °C		26.6 [0.83]	27.2 [1.72]	25.5 [1.86]	25.7 [0.69]	24.3 [3.17]	21.7 [0.34]
		pH 10 buffer		26.6 [3.86]	25.5 [1.17]	26.8 [0.55]	25.4 [0.83]	24.1 [0.83]	23.1 [2.21]
TVM3408	2	Water at 23 °C	16.1 [1.17]	13.0 [1.24]	12.3 [0.76]	12.6 [2.55]	15.7 [1.59]	14.2 [0.41]	14.2 [0.28]
		Water at 60 °C		11.8 [2.21]	14.4 [1.79]	14.3 [2.07]	16.5 [4.62]	12.6 [3.45]	11.5 [3.31]
		pH 10 buffer		11.1 [0.48]	12.2 [0.83]	15.2 [1.10]	14.0 [1.31]	15.7 [1.86]	15.2 [2.00]
	4	Water at 23 °C	15.7 [0.14]	14.7 [0.90]	12.1 [1.03]	13.9 [1.31]	15.2 [1.25]	15.9 [1.25]	15.1 [0.21]
		Water at 60 °C		15.9 [2.00]	15.4 [0.83]	15.2 [1.31]	15.9 [1.45]	16.0 [1.03]	14.6 [0.62]
		pH 10 buffer		12.3 [0.28]	12.5 [0.34]	12.8 [1.31]	15.4 [1.31]	14.7 [1.38]	13.9 [1.46]

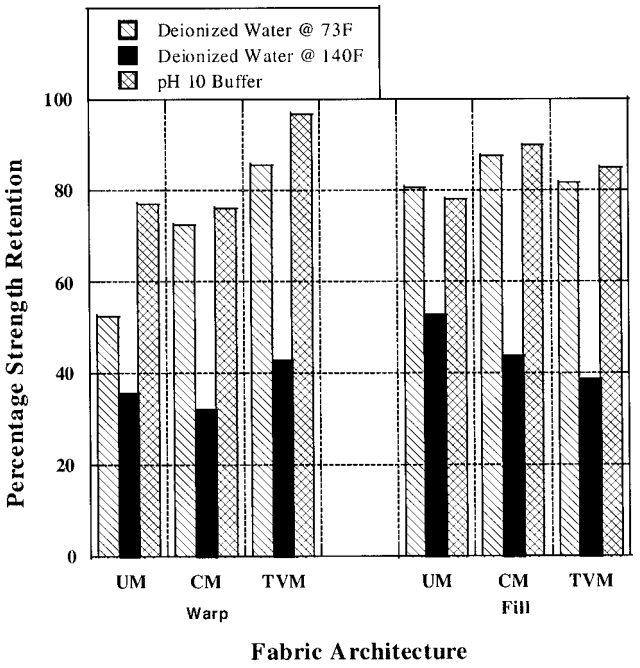

(a)

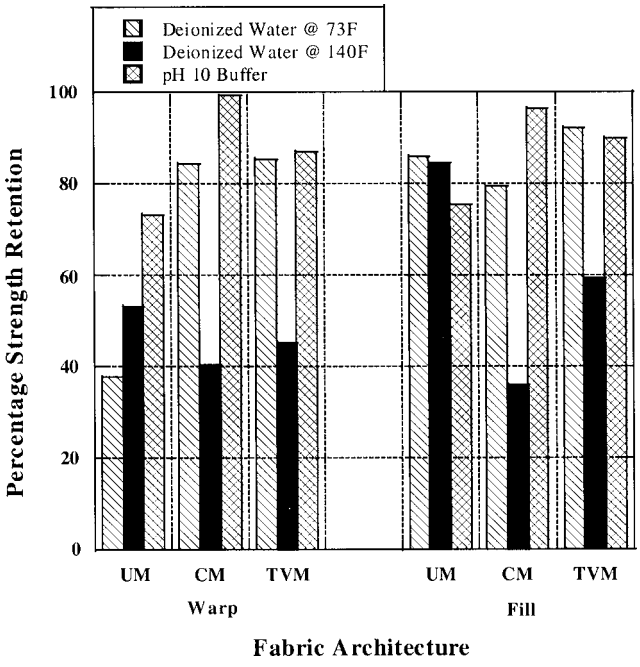

(b)

Figure 5. Percentage retention of tensile strength at the end of the 57 week exposure period: (a) 2 layered composites; (b) 4 layered composites.

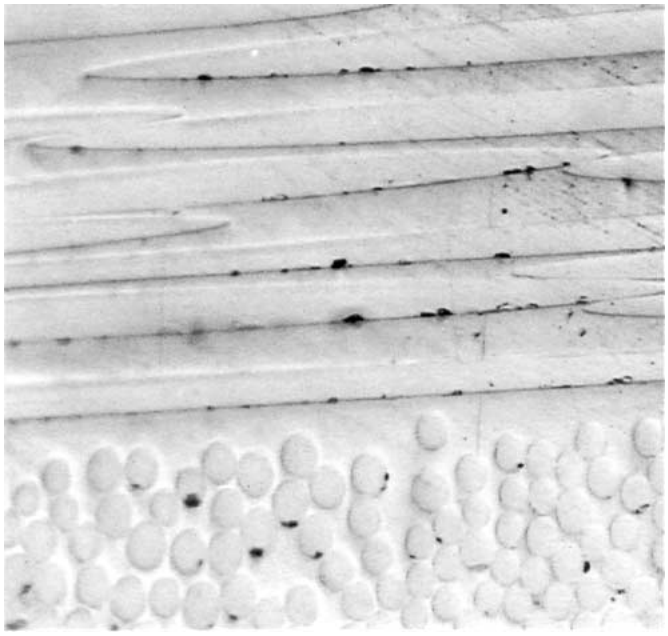

(a)

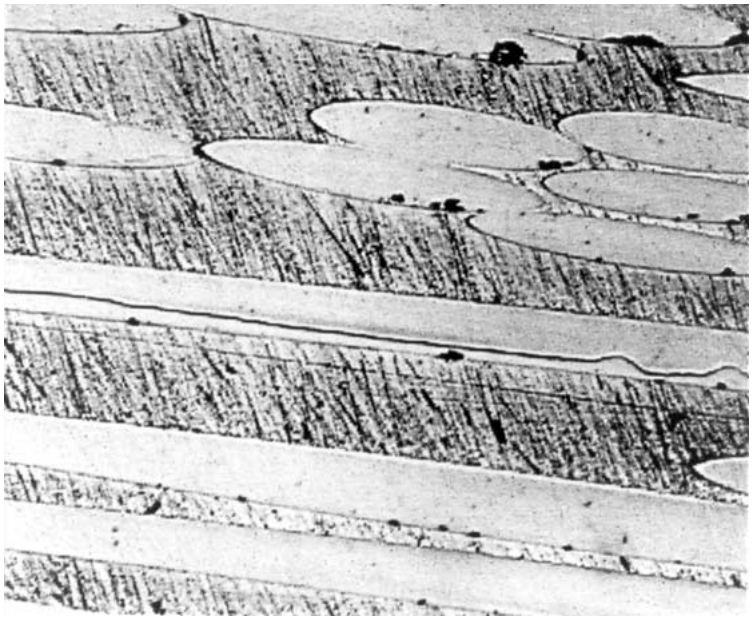

(b)

Figure 6. (a) Interface degradation and fiber pitting after immersion in deionized water for 57 weeks at 73 °F; (b) interface degradation, fiber pitting and cracking after immersion in deionized water for 57 weeks at 140 °F.

ages. The chemical attack, hydrolysis, although primarily a phenomenon associated with long periods of exposure, is also initiated by incomplete cure of the vinylester. Both plasticization and hydrolysis induce higher levels of molecular mobility resulting in consequent drop in T_g, although the drop can be partially offset through the residual curing of the vinylester itself in the aqueous solution. From Tables III and IV it can be seen that, in general, after immersion in deionized water at 23 °C (73 °F) and in the pH 10 buffer solution, strength decreases rapidly in the first few weeks and then increases due to effects of continuing increase in cross link density following trend earlier identified in [16, 24]. In some cases this increase is even to levels above the initial strength measured for the unexposed specimens. A plot showing changes in tensile strength in the warp direction for the 2 layered uniaxial (UM2403) specimens as a function of immersion solution and time is shown in Figure 7a. The effects of residual/post-cure (as shown through an apparent increase in level of tensile strength) are seen at the end of the first week and appear to taper off between 8 and 12 weeks. These results are corroborated by results of differential scanning calorimetry, which indicate substantial decrease in levels of residual heat indicating an increase in degree of polymerization over the period in which the residual cure is hypothesized to occur. Due to the competing effects of these phenomena causing both degradation and increase in network formation, the level of each is critical to the result. Immersion in water at 60 °C causes an acceleration in degradation which overshadows the effect of residual cure. Polymer systems such as polyesters and vinylesters, which contain styrene, are known to undergo rapid and local homopolymerization during cure resulting in composites not attaining complete cure/polymerization even after short periods of elevated temperature post-cure. As noted in [31, 32] the generic network formation in vinylesters can be considered as a combination of three ongoing reactions, namely the homopolymerizations of vinylester and styrene, and their copolymerization. Although the rate of fractional conversion of styrene double bonds is initially less than that of the vinylester, the styrene monomer continues reacting after the vinylester double bond conversion has stopped. This difference in rates results in microgel structure formation with areas of cross-link density being dispersed in pools of unreacted monomer. The systems can undergo thus slow residual curing over time. Insofar as immersion in solution is concerned, however, it should be noted that there are two competing mechanisms, namely those of auto acceleration and moisture induced residual-/post-cure causing an increase in cross-link density and glass transition temperature as previously identified in [16, 24, 33] which can also cause resin embrittlement, and the degradation of the resin and fiber-matrix bond through desorption of free low-molecular weight components which can be leached out of polymer segments which can lead to polymer flexibilization as noted in [34]. It is not clear at this point as to the relative contribution of each mechanism within the prior mentioned interim time period within which properties appear to increase and then decrease again. Further research is needed to identify and characterize these phenomena since they obviously are not included

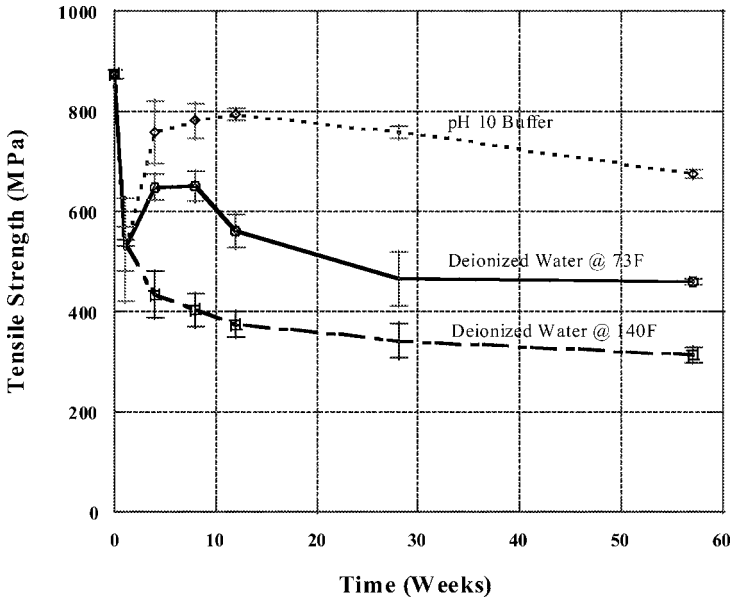

(a)

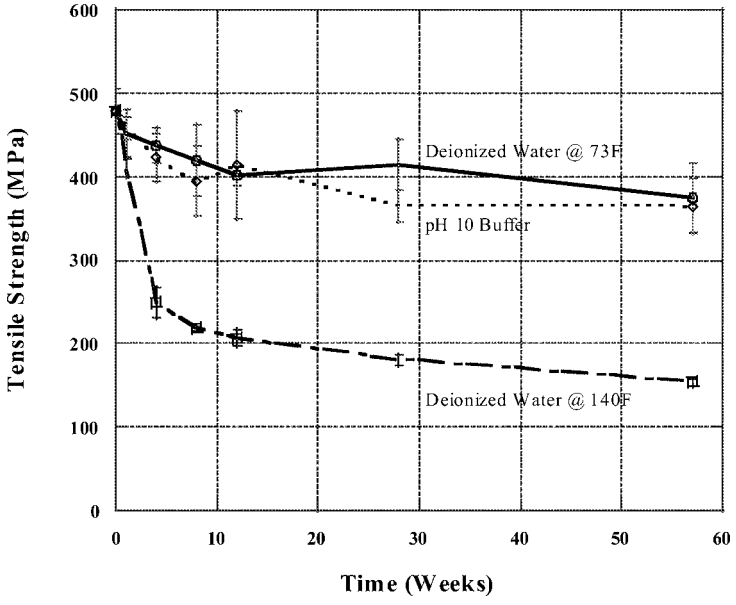

(b)

Figure 7. Effect of exposure on tensile characteristics of 2 layered composite tested in the warp direction: (a) UM2403; (b) CM5005.

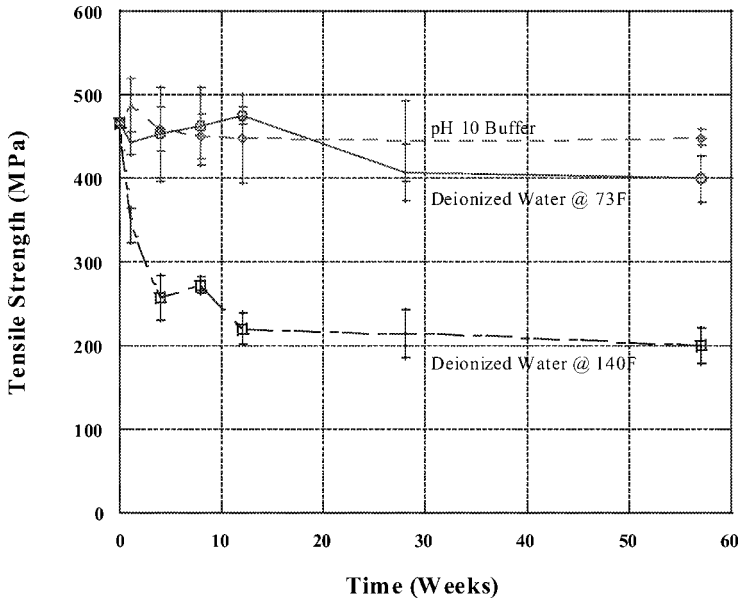

(c)

Figure 7. (Continued.) (c) TMV3408.

in the aging and stress-corrosion models based on separation of zero-stress aging from those of fiber level crack initiation and rapid progression as discussed by Haslor *et al*. [35], France [36] and Schultheisz *et al.* [37].

Although the level and rate of strength reduction are roughly the same for all three exposure types in the first week for the uniaxial composite tested in the warp direction (Figure 7a), this pronounced increase is not seen in either the biaxial, as in Figure 7b, or the triaxial, as in Figure 7c, specimens. In each of these there is not only a difference in the initial rate and level of strength degradation, but also a difference in the extent and time period of immersion induced post-cure. It is noted that the differences are further exemplified by thickness with the time for initial degradation being longer with increase in thickness and the apparent extent of post-cure being smaller.

Although differences in percentage retention of strength based on test direction (warp or fill) are to be expected, these effects are significant only in the uniaxial specimens wherein the warp direction is clearly associated with the fiber dominated direction and the fill direction is clearly resin dominated. The differences in response over the time period under consideration are shown in Figure 8. It is seen that the extent of post-cure, as noted through attendant increases in tensile strength, is far more significant in the fill direction both in terms of duration of time-period of attainment and in the extent of post-cure. For example in the first week of immersion in deionized water at 23 °C (73 °F) specimens in the warp direction are reduced in strength by 39.9% whereas those in the fill direction are reduced by

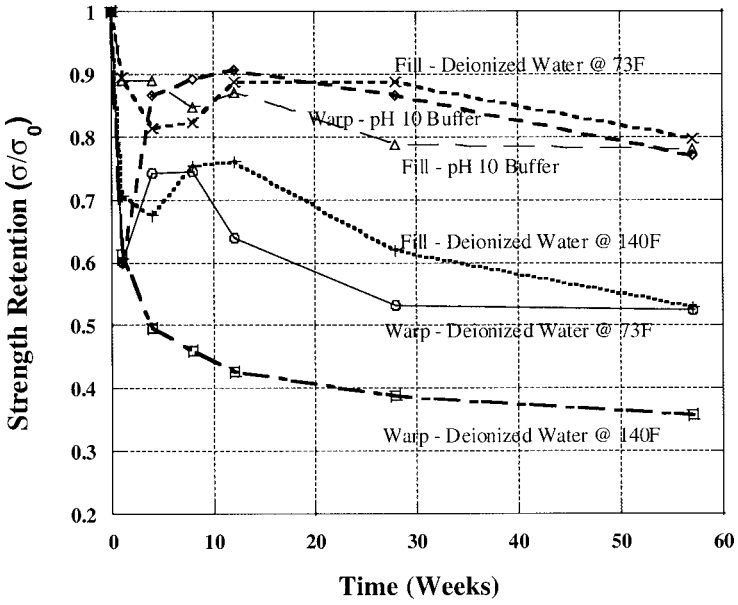

Figure 8. Strength retention for the 2 layered uniaxial specimens.

only 10.7%. After a period of twenty-six weeks the specimens in the warp direction have clearly been dominated by mechanisms of degradation with the reduction in strength being 46.8%, whereas those in the fill direction have been reduced by only 11.3%. The role of the resin is also clearly demonstrated in that the specimens in the fill direction immersed in deionized water at 60 °C (140 °F) show a clear indication of post-cure, in the period between 4 and 26 weeks, whereas no apparent effects of post-cure are seen in the warp direction in this case.

Results related to activation energies and diffusion coefficients in the previous section clearly show the acceleration effect due to increase in temperature of deionized water from 23 °C (73 °F) to 60 °C (140 °F). Tables III and IV and Figures 5 and 7 also show that immersion in deionized water at 60 °C (140 °F) results in significantly higher levels of degradation of tensile strength. It can be seen from Figure 7 that the rate of approach to the initial asymptote is more rapid at the elevated temperature level.

Of late, increasing attention has been paid to the investigation of high pH alkali solutions on property degradation of E-glass composites, especially as related to composite rebar embedded in concrete, and E-glass composites used for the external strengthening of concrete structural elements. It is important to emphasize at this point that the accelerated degradation of E-glass fibers by concrete pore solutions cannot be mimicked merely by high pH levels but is actually dependent on both pH and chemical content [26]. A comparison of effects due to the pH buffer used in this investigation, which is potassium based, and actual concrete based alkali solutions is given in [38] and hence will not be repeated herein. As

can be seen from Tables III and IV and Figures 5, 7 and 8, effects of the pH 10 buffer in the warp direction are less than those even from deionized water at 23 °C (73 °F), whereas in the fill direction the effects although often more than those from deionized water at 23 °C (73 °F) are less than those of deionized water at 60 °C (140 °F). Levels of damage seen after a period of 26 weeks are similar to those seen from immersion in water at 23 °C (73 °F), in that local fiber fracture and pitting is seen. At the level of 57 weeks, however, extensive degradation in the form of fiber degradation through longitudinal splitting close to the fiber-matrix interface (Figure 9a) and fiber-matrix interphase degradation with cracks penetrating transversely through the fiber (Figure 9b) are seen. It is noted that unlike the effects reported in [26] where degradation at the interface level was extensive, the degradation due to the pH buffer appears to be predominantly at the fiber level. Although this provides an indication of higher strength retention over the time period under consideration it is likely that the local fiber degradation will become more extensive and connected over time resulting in unstable crack growth at some future point, resulting in sudden and rapid strength degradation.

Typically, the immersion of E-glass composites in water results in a reduction in strength of between 20% and 80% depending on the period of immersion, fiber orientation, and solution temperature. Norwood and Marchant reported a decrease in strength between 20% and 50% with increasing exposure time for E-glass/polyester composites in water at 32 °C (90 °F) [39]. The overall trends in terms of reduction in strength with the initial period being the most critical are clearly seen from the results described earlier. In general, previous investigations have reported significantly low levels of reduction in modulus for these composites, and this trend is largely followed in the results of the current investigation. As can be seen from Tables V and VI and Figure 10 the reduction in modulus was at the maximum 28.4% corresponding to the 2-layered triaxial (TVM3408) specimens tested in the fill direction after immersion in deionized water at 60 °C (140 °F). It is also seen that the 2-layered specimens show a higher degree of modulus loss than the 4-layered samples. As can be seen from Tables V and VI there is some evidence of aqueous solution initiated post-cure with the phenomenon ranging over varying periods of time depending on sample thickness, fiber orientation, and direction. The effects of post-cure on strength are clearly more pronounced in the fill direction with intermediate levels at times being higher than the unexposed values. The CM5005 2-layered specimens for example tested in the fill direction show an initial modulus of 26.34 GPa whereas after 12 weeks of immersion in water at 23 °C (73 °F) they show a modulus of 28.34 GPa, an increase of 7.6%. In comparison the warp direction specimens show a decrease of 18.3% after the same time period. The reader is cautioned, however, that although the effects on modulus appear to be relatively small, these reductions are likely to increase dramatically at some point in the future corresponding to the increasing level of damage to the fiber resulting from notching, spiral and longitudinal cracking, and even fragmentation.

(a)

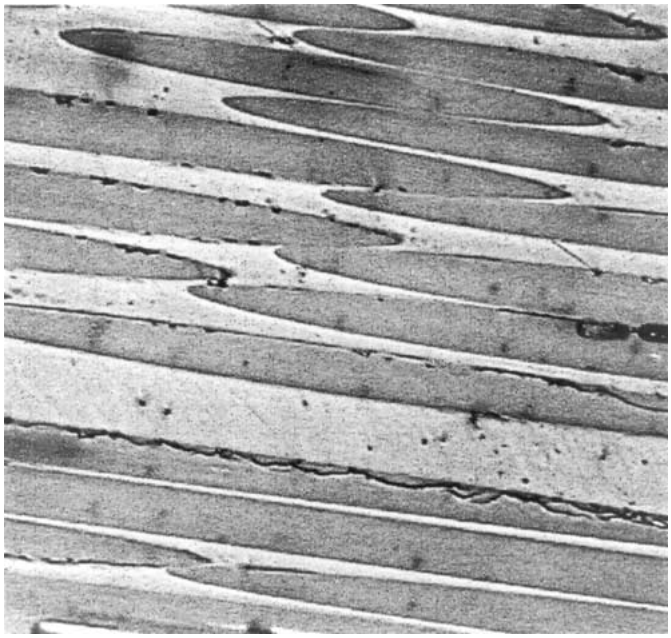

(b)

Figure 9. Degradation due to immersion in a pH 10 buffer at the fiber, and fiber-matrix interphase level.

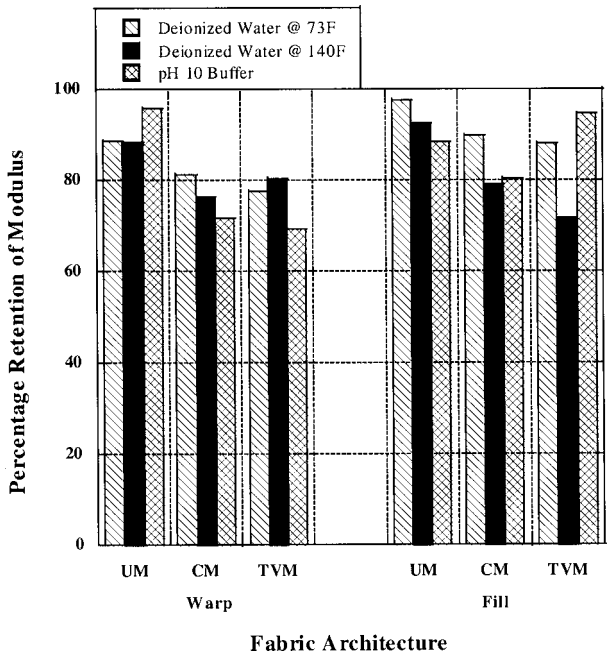

(a)

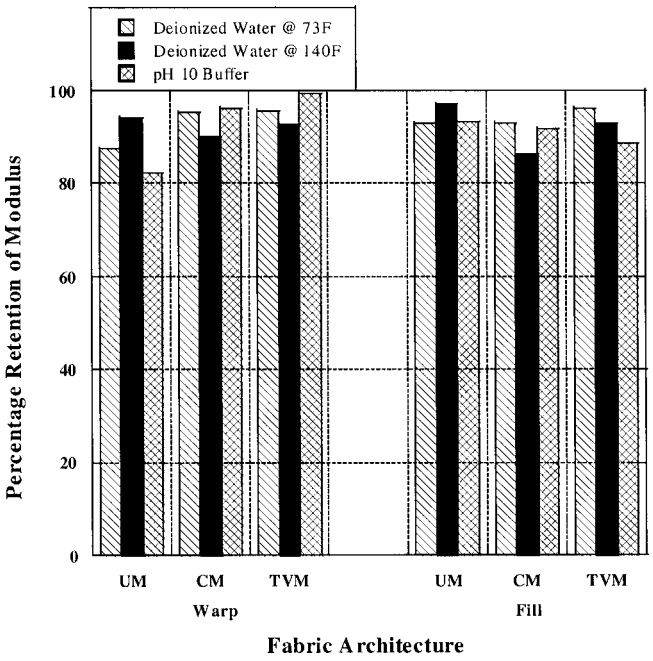

(b)

Figure 10. Percentage retention of tensile modulus at the end of the 57 week exposure period: (a) 2 layered composites; (b) 4 layered composites.

Table VII. Overall results of short beam shear strength (MPa) characterization.

Direction	Fabric	Exposure	Time of immersion						
			Unexposed	1 week	4 weeks	8 weeks	12 weeks	26 weeks	57 weeks
Warp	UM2403	Water at 23 °C	57.9 [2.14]	49.0 [1.45]	50.0 [2.28]	49.9 [4.34]	48.6 [1.79]	50.6 [0.76]	50.1 [0.28]
		Water at 60 °C		53.0 [2.14]	50.2 [1.59]	46.8 [1.93]	48.8 [3.03]	44.7 [7.72]	43.8 [5.72]
		pH 10 buffer		51.7 [0.90]	46.1 [4.41]	50.8 [2.96]	52.8 [1.59]	51.2 [2.48]	49.0 [1.79]
	CM5005	Water at 23 °C	42.5 [1.38]	39.5 [1.86]	37.8 [1.52]	39.7 [1.45]	38.3 [1.52]	40.3 [4.76]	39.1 [3.72]
		Water at 60 °C		40.6 [1.52]	42.5 [0.83]	41.0 [2.55]	40.1 [2.62]	41.5 [1.03]	35.8 [1.24]
		pH 10 buffer		41.4 [3.72]	41.2 [4.34]	41.9 [0.76]	39.7 [1.72]	39.5 [3.86]	36.7 [5.10]
	TVM3408	Water at 23 °C	46.7 [4.14]	41.7 [4.07]	44.5 [3.95]	42.8 [3.86]	40.3 [5.10]	43.9 [1.79]	41.3 [2.55]
		Water at 60 °C		41.3 [3.65]	39.4 [6.07]	36.6 [0.83]	37.4 [0.83]	33.4 [2.21]	31.2 [1.93]
		pH 10 buffer		45.1 [2.34]	46.5 [2.07]	46.3 [3.10]	45.6 [4.90]	39.5 [3.86]	34.8 [2.55]
Fill	UM2403	Water at 23 °C	16.8 [0.76]	12.8 [0.41]	12.8 [0.21]	13.17 [0.48]	13.45 [1.79]	8.55 [0.76]	7.93 [0.28]
		Water at 60 °C		11.9 [1.03]	8.7 [1.45]	7.0 [1.59]	7.9 [0.69]	8.1 [0.76]	7.7 [2.07]
		pH 10 buffer		12.82 [0.69]	16.9 [2.69]	13.0 [2.21]	12.8 [2.34]	12.6 [0.62]	11.6 [2.55]
	CM5005	Water at 23 °C	36.3 [3.17]	30.5 [2.96]	39.2 [3.72]	34.5 [5.72]	35.4 [6.55]	34.1 [5.72]	34.6 [0.07]
		Water at 60 °C		41.3 [2.69]	38.4 [1.52]	36.8 [3.52]	38.5 [3.52]	37.6 [4.76]	34.5 [2.48]
		pH 10 buffer		42.7 [4.96]	39.7 [2.96]	37.4 [1.03]	37.6 [2.00]	37.7 [2.28]	36.3 [2.76]
	TVM3408	Water at 23 °C	31.9 [0.48]	29.7 [2.00]	31.6 [1.24]	32.8 [2.07]	32.2 [1.31]	31.7 [2.21]	29.3 [0.97]
		Water at 60 °C		29.6 [1.17]	28.7 [3.79]	28.9 [1.86]	27.7 [0.48]	27.1 [2.07]	25.1 [1.79]
		pH 10 buffer		30.1 [2.21]	30.3 [1.79]	27.9 [1.93]	28.4 [2.21]	27.6 [3.17]	26.4 [3.38]

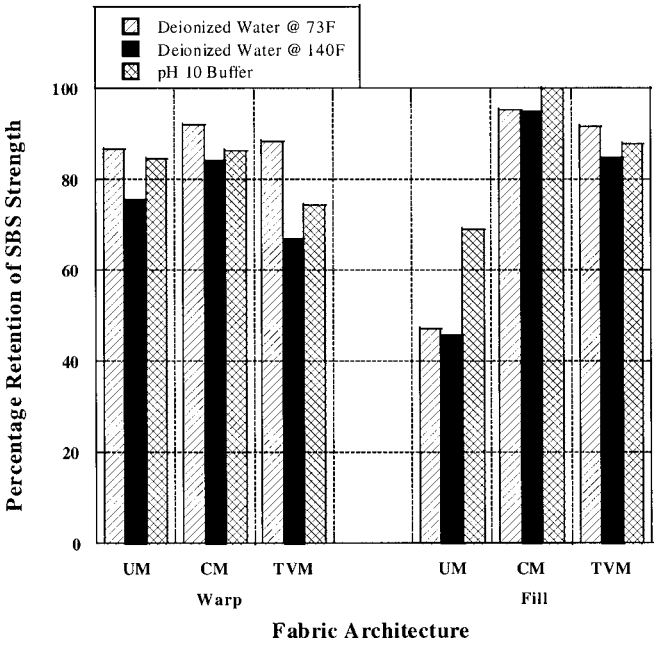

Figure 11. Percentage retention of apparent shear strength (sbs) at the end of the 57 week exposure period.

3.3. SHORT-BEAM-SHEAR CHARACTERIZATION

In order to avoid test fixture induced crushing which is common in thin specimens, short-beam-shear tests were only conducted on the four-layered specimens, results of which are given in Table VII. It should be noted that optical microscopy of earlier specimens did not show any sign of delamination or separation between layers and hence it was expected that there would be a significant level of retention of short-beam-shear strength even after the severe exposure due to immersion in deionized water at 60 °C (140 °F). As seen in Figure 11, with the exception of the uniaxial specimens tested in the fill direction, reductions of 5% to 33.2% were noted. The larger drop in the uniaxial specimens tested in the fill direction can be related to the absolute lack of fibers in the transverse direction and the presence of either debonds or longitudinal cracks in fibers in the longitudinal direction which in essence lie perpendicular to the short-beam-shear specimen test span thereby creating a number of weak zones along which transverse cracking could easily take place during testing. Overall the largest reduction was seen in specimens immersed in deionized water at 60 °C (140 °F), which follows the trend seen through tensile characterization. From Figure 11 it can be seen that the biaxial specimens have higher interlaminar shear strength retention than the other specimens, which is in agreement with the earlier results reported, by Dukes and Griffiths [40].

3.4. DMTA CHARACTERIZATION

Dynamic Mechanical Thermal Analysis (DMTA) conducted immediately after initial conditioning showed that the glass transition temperatures ranged from 227–230 °F for all the specimens, with T_g rising to 246–249 °F after 8 weeks of immersion in solution. Tests conducted after the full period of immersion indicated that in all cases immersion in deionized water at 73 °F and the pH 10 buffer resulted in a 5–7% reduction in glass transition temperature (determined as the point corresponding to the peak in the $\tan\delta$ curve) as compared to the initial level, whereas specimens immersed in deionized water at 140 °F showed a 10–15% drop. Small changes were also seen in the overall shape of the bending modulus (E') curves in that new plateaus and sub-maximal peaks were seen indicating initiation of changes in material structure. It should be noted that Ghorbel and Valentin [24] noted a similar drop of 9.45% in the glass transition temperature after exposure of E-glass/Vinylester composites to water at 140 °F.

4. Summary and Conclusions

The results presented in this paper describe the effects of short-term exposure of E-glass/Vinylester composites to three specific environments, and it is shown that effects are significantly different based on both thickness (due to the requirement of longer times to attain moisture equilibrium in thicker specimens) and orientation of fibers in the layup (due to combined effects of plasticization, relaxation of residual stresses, and fiber or interphase related damage modes). It is shown that damage takes place through interphase debonding and degradation as well as fiber pitting, spiral cracking and longitudinal cracking, each of which not only result in reduction of mechanical properties, but also serve as the means for renewed absorption of water resulting in moisture absorption to levels above the initial plateau. This two stage absorption is also accompanied by moisture induced post-cure of the specimens which results in an increase in levels of mechanical performance after the initial rapid drop due to immersion in an aqueous medium. This phenomenon in addition to the fiber level damage creates a challenge for modeling and prediction of long-term performance of these materials based on short-term (even at the level of 57 weeks) exposures.

Acknowledgements

The authors gratefully acknowledge the support of the Fluor Foundation for purchase of equipment. The support of the National Science Foundation CAREER program through award number 9702560 is also gratefully acknowledged. The authors would also like to thank an anonymous referee for detailed comments which resulted in the addition of substantial clarifications to an earlier version of this paper, which has, in the opinion of the authors, led to a paper that can be better understood to all levels of readers.

References

1. Karbhari, V. M., Chin, J. W., and Reynaud, D., 'Critical Gaps in Durability Data for FRP Composites in Civil Infrastructure', in *Proceedings of the 45th International SAMPE Symposium*, Long Beach, 2000, pp. 549–563.
2. Schutte, C. L., 'Environmental Durability of Glass-Fiber Composites', *Materials Science and Engineering* **R13**, 1994, 265–324.
3. Weitsman, Y. J., 'Effects of Fluids on Polymeric Composites – a Review', Report to Office of Naval Research, Mechanical and Aerospace Engineering and Engineering Science, University of Tennessee, Report MAES98-5.0-CM, August 1998.
4. Puccini, G., 'Environmental Aspects', in *Composite Materials in Maritime Structures*: Vol. 1, R. A. Shenoi and J. F. Wellicome (eds), Cambridge University Press, Cambridge, UK, 1993.
5. ASME-RTP-1d, 'Reinforced Thermoset Plastic Corrosion Resistant Equipment', American Society of Mechanical Engineers, New York, 1998.
6. Leiblein, S. 'Survey of Long-Term Durability of Fiberglass – Reinforced Plastic Structures', NASA Report CR-165320, January 1981, Rocky River, Ohio, pp. 52.
7. Harper, J. F. and Naeem, M., 'The Moisture Absorption of Glass Fibre Reinforced Vinylester and Polyester Composites', *Materials and Design* **10**(6), 1989, 297–300.
8. Juska, T., Williams, C., and Loup, D., 'Durability of GRP in a Marine Environment', NSWC Program, 1997.
9. Apicella, A., Migliaresi, C., Nicolais, L., Iaccarino, L., and Roccotelli, S., 'The Water Aging of Unsaturated Polyester-Based Composites: Influence of Resin Composite Structure', *Composites* **14**(4), 1983, 387–392.
10. Apicella, A., Migliaesi, C., Nicodemo, L., Nicolais, L., Iaccarino, L., and Roccotelli, S., 'Water Sorption and Mechanical Properties of a Glass-Reinforced Polyester Resin', *Composites* **13**, 1982, 406–410.
11. Bradley, S. W., Puckett, P. M., Bradley, W. L., and Sue, H. J., 'Viscoelastic Creep Characteristics of Neat Thermosets Reinforced with E-Glass', *Journal of Composites Technology and Research* **20**(1), 1998, 51–58.
12. Riffle, J. S., Lesko, J. J., and Puckett, P. M., 'Chemistry of Polymer Matrix Resins for Infrastructure', in *Fiber Composites in Infrastructure*, Vol. 1, H. Saadatmanesh and M. Ehsani (eds), 1998, pp. 23–34.
13. Karbhari, V. M. and Zhang, S., 'Durability of Fiber Reinforced Composites in Civil Infrastructure: Issues, Results and Implications', in *Proceedings of DURACOSYS 99*, Brussels, 1999, p. 12.
14. Chin, J. W., Nguyen, T., and Aouadi, K., 'Sorption and Diffusion of Water, Salt Water, and Concrete Pore Solution in Composite Matrices', *Journal of Applied Polymer Science* **71**, 1999, pp. 483–492.
15. Juska, T., Williams, C., and Loup, D., 'Durability of GRP in a Marine Environment', US Navy Carderock Division, unpublished report.
16. Marshall, J. M., Marshall, G. P., and Pinzelli, R. F., 'The Diffusion of Liquids into Resins and Composites', *Polymer Composites* **13**(3), 1982, 131–137.
17. Lagrange, A., Melennec, C., and Jacquemet, R., 'Influence of Various Stress Conditions on the Moisture Diffusion of Composites in Distilled Water and Natural Sea Water', in *Durability of Polymer Based Composite Systems for Structural Applications*, A. H. Cardon and G. Verchery (eds), Elsevier Applied Sciences, 1991, pp. 385–392.
18. Springer, G. S., Sanders, B. A., and Tung, R. W., 'Environmental Effects on Glass Fiber Reinforced Polyester and Vinylester Composites', in *Environmental Effects of Composite Materials*, G. S. Springer (ed.), Technomic Publishing Co., 1981, pp. 126–144.
19. Crank, J. and Park, G. S., *Diffusion in Polymers*, Academic Press, London, 1968.

20. Weitsman, Y. A., 'A Continuum Diffusion Model for Viscoelastic Materials', *Journal of Physical Chemistry* **94**, 1990, 961–968.
21. Gurtin, M. and Yatomi, C., 'On a Model for Two Phase Diffusion in Composite Materials', *Journal of Composite Materials* **13**, 1979, 126–130.
22. Carter, H. G. and Kibler, K. G., 'Langmuir-Type Model for Anomalous Moisture-Diffusion in Composite Resins', *Journal of Composite Materials* **12**, 1978, 118–131.
23. Cai, L. and Weitsman, Y., 'Non-Fickian Moisture Diffusion in Polymeric Composites', *Journal of Composite Materials* **28**(2), 1994, 130–154.
24. Ghorbel, I. and Valentin, D., 'Hydrothermal Effects on the Physico-Chemical Properties of Pure and Glass-Fiber Reinforced Polyester and Vinylester Resins', *Polymer Composites* **14**(4), 1993, 324–334.
25. Shen, C. H. and Springer, G. S., 'Moisture Absorption and Desorption of Composite Materials', *Journal of Composite Materials* **10**, 1976, 1–20.
26. Zhang, S. and Karbhari, V. M., 'Effects of Alkaline Environments on the Durability of E-Glass Fiber Composites for Use in Civil Infrastructure', in *Proceedings of the 14th Technical Conference of the American Society of Composites*, Fairborn, OH, 1999, pp. 12–19.
27. Karbhari, V. M. and Lee, R., 'On the Effect of E-Glass Fiber on the Cure Behavior of Vinylester Composites', *Journal of Reinforced Plastics and Composites*, 2001 (in press).
28. Wyatt, R. C. and Ashbee, K. H. G., 'Debonding in Carbon Fibre/Polyester Resin Composites Exposed to Water: Comparison with E-Glass Fibre Composites', *Fibre Science and Technology*, 1969, 29–40.
29. Ishai, O., 'Environmental Effects on Deformation, Strength, and Degradation of Unidirectional Glass-Fiber Reinforced Plastics. I. Survey', *Polymer Engineering and Science* **15**(7), 1975, 486–499.
30. Ehrenstein, G. W. and Spaude, R., 'A Study of the Corrosion Resistance of Glass Fibre Resin Polymers', *Composite Structures* **2**, 1984, 191–200.
31. Ziaee, S. and Palmese, G. R., 'Effects of Temperature on Cure Kinetics and Mechanical Properties of Vinyl-Ester Resins', *Journal of Polymer Science: Part B* **37**, 1999, 725–744.
32. Karbhari, V. M., Rivera, J., and Zhang, J., 'Low-Temperature Hygrothermal Degradation of Ambient Cured E-Glass/Vinylester Composites', submitted to *Journal of Applied Polymer Science*, 2001.
33. Ganem, M., Mortaigne, B., Bellenger, V., and Verdu, J., 'Hydrolytic Ageing of Vinyl Ester Materials Part 1. Ageing of Prepolymers and Model Compounds', *Polymer Networks and Blends* **4**(2), 1994, 87–92.
34. Chin, J. W., Aouadi, K., Haight, M. R., Hughes, W. L., and Nguyen, T., 'Effects of Water, Salt Solution and Simulated Concrete Pore Solution on the Properties of Composite Matrix Resins Used in Civil Engineering Applications', *Polymer Composites* **22**(2), 2001, 282–297.
35. Haslor, P., Jensen, K. B., and Skovgaard, N. H., 'Degradation of Stressed Optical Fibers in Water: New Worst-Case Lifetime Estimation Model', *Journal of the American Ceramic Society* **77**, 1994, 1531–1536.
36. France, P. W., Duncan, W. J., Smith, D. J., and Beales, K. J., 'Strength and Fatigue of Multicomponent Optical Glass Fibers', *Journal of Materials Science* **18**, 1983, 785–792.
37. Schultheisz, C. R., McDonough, W. G., Kondagunta, S., Schutte, C. L., Macturk, K. S., McAuliffe, M., and Hunston, D. L., 'Effect of Moisture on E-Glass/Epoxy Interfacial and Fiber Strengths', in *ASTM STP* 1242, 1997, pp. 257–286.
38. Zhang, S. and Karbhari, V. M., 'Effects of Alkaline Environments on the Durability of E-Glass Fiber Composites for Use in Civil Infrastructure', in *Proceedings of the 14th Technical Conference of the American Society of Composites*, Fairborn, OH, 1999, pp. 12–20.

39. Norwood, L. S. and Marchant, A., 'Recent Developments in Polyester Matrices and Reinforcements for Marine Applications, in Particular in Polyester/Kevlar Composites', *Composite Structures*, 1981, 158–181.
40. Dukes, R. and Griffiths, D. L., 'Marine Aspects of Carbon-Fibre and Glass-Fibre/Carbon-Fibre Composites', in *Proceedings of the International Conference on Carbon Fibers, their Composites and Applications*, Dorset, England, 1971.